Periodic orbits for the elliptic case of the Sun-Earth-Moon problem in new coordinates

A. Escalona-Buendía† and E. Piña‡
Departamento. de Física, Universidad Autónoma Metropolitana - Iztapalapa.
Apdo. Post. 55534. México, D. F. 09340, México.
†*aheb@xanum.uam.mx* ‡*pge@xanum.uam.mx*

Recibido el 29 de abril de 2002; aceptado el 17 de junio de 2002

We present a set of periodic and quasi-periodic orbits for the bidimensional case of the Sun-Earth-Moon problem using the coordinates recently introduced by Piña and Jiménez-Lara. Eliminating the restriction we used in a previous work that Earth-Moon system describes a circular orbit around the Sun, we recover the periodic orbits we have found, and we find periodic orbits for the elliptic case. We also find quasi-periodic orbits closer to the real case.

Keywords: Three body problem; Moon theory; celestial mechanics.

Presentamos un conjunto de órbitas periódicas y cuasi-periódicas para el caso bidimensional del problema Sol-Tierra-Luna, utilizando las coordenadas recientemente propuestas por E. Piña y L. Jiménez-Lara. Eliminando la restricción que habíamos utilizado en un trabajo anterior, de que el sistema Tierra-Luna describe una órbita circular en torno al Sol, recuperamos las soluciones periódicas que habíamos encontrado y encontramos soluciones periódicas para el caso elíptico; además de órbitas cuasi-periódicas cercanas al caso real.

Descriptores: Problema de tres cuerpos; teoría lunar; mecánica celeste.

PACS: 46.10.-z; 95.10.Ce; 96.20.-n

1. Introduction

In Ref. 1 we shown a first approach to the Sun-Earth-Moon problem. We imposed the restriction that the Earth-Moon subsystem performs a uniform circular motion around the Sun. With that simplification, the problem is reduced into a system with two degrees of freedom. This allowed to use the technique of the symmetry lines to search for periodic orbits.

For this work we have removed that restriction. The system has three degrees of freedom, so the symmetry lines technique is not applicable. However, we can use some of the symmetry properties of the system to help us in the search for periodic orbits. Perturbing these periodic orbits, we search for solutions whose behavior resemble, under the bidimensional approximation, the real orbit.

We present a classification of the solutions in accordance with the trajectory of the Earth-Moon subsystem around the Sun, and with the trajectory of the Moon around the Earth. Finally, we make qualitative comparing between our numerical solutions and the astronomical data.

2. System of coordinates

Let m_1, m_2, m_3 be the masses of Sun, Earth and Moon, respectively. The new set of coordinates is defined in a non-inertial reference system, parallel to the directions of the principal inertia axes of the triangle described by the three bodies, with the origin at the barycenter [2, 3]. Let $\mathbf{s}_1, \mathbf{s}_2, \mathbf{s}_3$ be the positions of Sun, Earth and Moon respectively in this rotating frame, and $\mathbf{r}_1, \mathbf{r}_2, \mathbf{r}_3$ be the corresponding positions in an inertial system; the transformation from one frame into the other is made by a rotation matrix, $\mathbf{r}_i = \mathbf{G}\mathbf{s}_i$. The problem is restricted to the bidimensional case, so we need just one Euler angle ψ.

The selection of the reference system makes the matrix of inertia to be diagonal; because three particles conform a plane, just two of the moments of inertia are independent: $I_3 = I_1 + I_2$. Piña and Jiménez-Lara define two coordinates R_1, R_2 with dimensions of length related to these moments of inertia [3]:

$$I_1 = \mu R_1^2, \tag{1}$$

$$I_2 = \mu R_2^2, \tag{2}$$

where

$$\mu = \sqrt{\frac{m_1 m_2 m_3}{m_1 + m_2 + m_3}}. \tag{3}$$

There is another coordinate, an angle σ related to the geometry of the system. The details of the development of σ are presented in Refs. 2 and 3. Let p, q, r be the distances Earth-Moon, Sun-Moon, and Sun-Earth respectively. The relation for the new coordinates and the distances is

$$\begin{pmatrix} p^2 \\ q^2 \\ r^2 \end{pmatrix} = \mathbf{B} \begin{pmatrix} R_1^2 \sin^2\sigma + R_2^2 \cos^2\sigma \\ R_1^2 \cos^2\sigma + R_2^2 \sin^2\sigma \\ 2(R_2^2 - R_1^2)\sin\sigma\cos\sigma \end{pmatrix}, \tag{4}$$

where matrix $\mathbf{B}$ depends on the masses of the particles only.

We presented a redefinition of σ in [1] making use of the properties of the Sun-Earth-Moon case: $m_1 \gg m_2 > m_3$, $q \cong r \gg p$. The only change takes place in the explicit form of $\mathbf{B}$.

$$\mathbf{B} = \frac{1}{m_2 + m_3} \begin{pmatrix} 0 & \frac{(m_2+m_3)^2}{\sqrt{m_2 m_3}} & 0 \\ \sqrt{m_2 m_3} & \frac{m_2^2}{\sqrt{m_2 m_3}} & m_2 \\ \sqrt{m_2 m_3} & \frac{m_3^2}{\sqrt{m_2 m_3}} & -m_3 \end{pmatrix} + O(1/m_1). \tag{5}$$

This new σ describes small oscillations around zero.

From Eq. (4), is easy to make estimations of the order of magnitude of the three variables: The amplitude of the oscillations for σ are very small, less than one minute of arc. R_1 and R_2 can be estimated by

$$R_1^2 \leq \frac{\sqrt{m_2 m_3}}{m_2+m_3} p^2, \quad (6)$$

$$R_2^2 + R_1^2 \cong \frac{m_2+m_3}{\sqrt{m_2 m_3}} r^2. \quad (7)$$

2.1. Astronomical data

Figures 1a and 1b show successive values for R_1 and σ calculated from the astronomical data of July, 2001 [4, 5], ignoring the angle between the Moon's orbit and the ecliptic. We can see that there is a phase locking between R_1 and σ:

- The zeroes of R_1 match with the extreme values of σ when the three particles are collinear. Restricted to the bidimensional case, a collinear configuration takes place at full moon and new moon; the 5^{th} and 20^{th} days, respectively.

- The zeroes of σ and the extreme values of R_1 occurs when the Moon is at first and third quarter, 13^{th} and 27^{th} days respectively, when the system describes an isosceles triangle.

The evolution of R_2 is very slow, in the same interval it starts in 3.07095 AU, reaches a maximum in 3.07100 and decreases monotonously to 3.06610. As we can see from Eq. (7), the behavior of R_2 is dominated by the Sun-Earth distance, so its period is close to the sidereal year. The period for R_1 is the lunar month, that is the time between consecutive full moons, so the system is quasi-periodic. The quotient of these periods is 12.368, it is the basis for the division of the year in 12 months of 28 to 31 days of the Jewish calendar [6].

3. Hamiltonian formalism

As we shown in Ref. 1, the Hamiltonian function of the system is given by

$$H = \frac{1}{2\mu}[P_1^2 + P_2^2 + \frac{R_1^2+R_2^2}{(R_1^2-R_2^2)^2}(P_\sigma^2 + P_\psi^2) + 4\frac{R_1 R_2}{(R_1^2-R_2^2)^2} P_\sigma P_\psi] + V, \quad (8)$$

where

$$V = -Gm_1m_2m_3(\frac{1}{m_1 p} + \frac{1}{m_2 q} + \frac{1}{m_3 r}).$$

By Hamilton equations, the relationship of the canonical moments with the canonical coordinates and their derivatives is given by

$$P_1 = \mu \dot{R}_1, \quad (9)$$

$$P_2 = \mu \dot{R}_2, \quad (10)$$

$$P_\sigma = \mu(R_1^2+R_2^2)\dot{\sigma} - 2\mu R_1 R_2 \dot{\psi}, \quad (11)$$

$$P_\psi = \mu(R_1^2+R_2^2)\dot{\psi} - 2\mu R_1 R_2 \dot{\sigma}. \quad (12)$$

Is easy to verify that P_ψ is a constant of motion, the angular momentum, so we handle it as a parameter of the system rather that a canonical variable. The system is conservative, so the energy $E = H(R_1, R_2, \sigma, P_1, P_2, P_\sigma)$ is also a constant of motion.

4. Symmetries

Analogously as we did in Ref. 1 with the technique of the symmetry lines, we make use of the symmetry properties of the system to search for periodic orbits.

Let be a Poincaré section defined by $R_1 = 0$, *i.e.*, collinear configuration; on this surface, P_1 can be written in terms of the other variables:

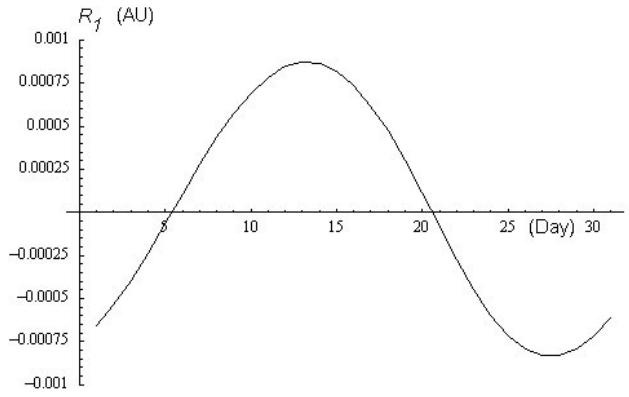

FIGURE 1a. R_1. Astronomical data.

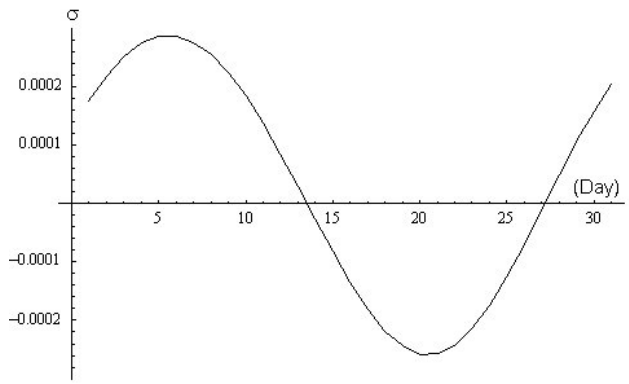

FIGURE 1b. σ. Astronomical data.

$$P_1^2 = 2\mu(E-V) - P_2^2 - \frac{P_\sigma^2 + P_\psi^2}{R_2^2}. \tag{13}$$

There is an ambiguity in the sign of P_1, so let be:

- Σ_+, the surface of section defined by $R_1 = 0, P_1 > 0$.
- Σ_-, the surface of section defined by $R_1 = 0, P_1 < 0$.

We have choose, arbitrarily, associate the full moon configuration with $P_1 > 0$, and the new moon with $P_1 < 0$.

This is a reversible system, the Hamiltonian function is invariant under the transformation

$$\mathbf{I}_0 \begin{pmatrix} R_1 \\ R_2 \\ \sigma \\ P_1 \\ P_2 \\ P_\sigma \end{pmatrix} = \begin{pmatrix} -R_1 \\ R_2 \\ \sigma \\ P_1 \\ -P_2 \\ -P_\sigma \end{pmatrix}. \tag{14}$$

This transformation is an involution, *i.e.*, $\mathbf{I}_0\mathbf{I}_0 = \mathbf{1}$.

On the surfaces of section Σ, let be Γ_0 the set of points invariant under $\mathbf{I}_0$, this means $\Gamma_0 = \mathbf{I}_0\Gamma_0$:

$$\Gamma_0^+ = \{\chi \in \Sigma_+ | P_2 = 0, P_\sigma = 0\}, \tag{15}$$

$$\Gamma_0^- = \{\chi \in \Sigma_- | P_2 = 0, P_\sigma = 0\}. \tag{16}$$

Let be ϕ_t the flow defined by the integration of the equations of motion, $\phi_t\chi(t_0) = \chi(t_0 + t)$. It is a canonical transformation, other properties of ϕ_t are

$$\phi_{s+t} = \phi_s\phi_t, \tag{17}$$

$$\phi_t\phi_{-t} = \mathbf{1}. \tag{18}$$

Because of the reversibility of the system we can write [7]

$$\phi_{-t} = \mathbf{I}_0\phi_t\mathbf{I}_0. \tag{19}$$

The last equation is valid for any time interval, finite or infinitesimal. Let be $\mathbf{T} : \Sigma_+ \to \Sigma_+$ a Poincaré mapping; written in terms of the flow:

$$\mathbf{T}\chi = \phi_\tau\chi = \chi'', \tag{20}$$

for some time interval τ, and χ, $\chi'' \in \Sigma_+$.

Let be **T** = **R S** a factorization in two semimappings [8] such that

$$\mathbf{S} : \Sigma_+ \to \Sigma_-, \tag{21}$$

$$\mathbf{R} : \Sigma_- \to \Sigma_+. \tag{22}$$

In this way $\mathbf{S}\ \chi = \phi_{\tau_1}\chi = \chi'$, $\mathbf{R}\ \chi' = \phi_{\tau_2}\chi' = \chi''$; where $\chi, \chi'' \in \Sigma_+$, $\chi' \in \Sigma_-$, and $\tau = \tau_1 + \tau_2$.

By Eq. (19),

$$\mathbf{I}_0\phi_{\tau_1}\mathbf{I}_0\chi' = \phi_{-\tau_1}\chi' = \chi, \tag{23}$$

$$\phi_{\tau_1}\mathbf{I}_0\chi' = \mathbf{I}_0\chi. \tag{24}$$

Since $\mathbf{I}_0\chi' \in \Sigma_-$ and $\mathbf{I}_0\chi \in \Sigma_+$, by definition of the semimapping **R**, the last equation can be written as

$$\mathbf{R}\mathbf{I}_0\chi' = \mathbf{I}_0\chi. \tag{25}$$

So we get $\mathbf{I}_0\mathbf{R}\mathbf{I}_0\mathbf{S}\chi = \chi$, which means

$$\mathbf{I}_0\mathbf{R}\mathbf{I}_0 = \mathbf{S}^{-1}. \tag{26}$$

Analogously

$$\mathbf{I}_0\mathbf{S}\mathbf{I}_0 = \mathbf{R}^{-1}. \tag{27}$$

Let $\chi \in \Gamma_0^+$ be an initial condition that evolves into a point $\chi' \in \Gamma_0^-$, by Eq. (26) we can write

$$\mathbf{R}\mathbf{I}_0\chi' = \mathbf{I}_0\mathbf{S}^{-1}\chi' = \mathbf{I}_0\chi. \tag{28}$$

Since χ and χ' are invariant under $\mathbf{I}_0$ we finally get

$$\mathbf{R}\chi' = \chi = \mathbf{T}\chi. \tag{29}$$

Therefore, the orbit is periodic.

By Eq. (11) the border conditions $R_1 = 0$, $P_\sigma = 0$ implies $\dot{\sigma} = 0$, i.e. there is phase locking between R_1 and σ. The Γ_0 are defined in collinear configuration and the extreme values of R_2; as is suggested by (7), the maximum and minimum of R_2 take place at aphelion and perihelion respectively. .

5. Circular case

In Ref. 1 we shown a first approach to the problem: We found a relation between the distance from the barycenter of the Earth-Moon subsystem to the Sun, R, and our coordinates:

$$R_1^2\sin^2\sigma + R_2^2\cos^2\sigma = \frac{m_2 + m_3}{\sqrt{m_2 m_3}}R^2. \tag{30}$$

Because the eccentricity of Earth's orbit around the Sun is small, we added the hypothesis that

$$R = \text{constant}.$$

This is the same hypothesis used by Hill [6, 9, 10]. Imposed as a restriction, it reduces the behavior of R_2 to small oscillations around a constant value, the amplitude of the oscillations is smaller than 1.1×10^{-7} AU.

When the restriction on R is removed, but keeping the same initial conditions, R remains constant along the numerical integration, so we recover the same periodic orbits. Figures 2a and 2b show the values of R_1 and σ respectively for a solution with a period of 27.465 days. The horizontal axis indicates the number of integration steps, h = 1/4096 sidereal years.

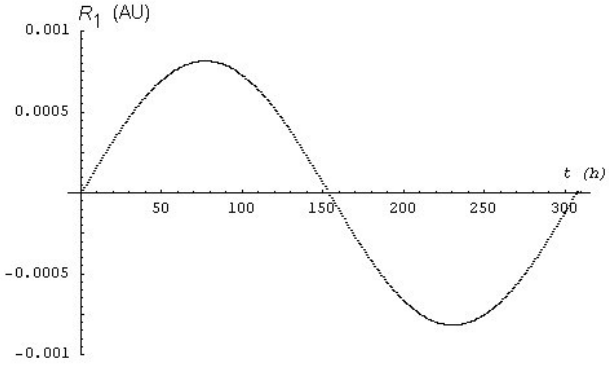

FIGURE 2a. R_1. Circular case.

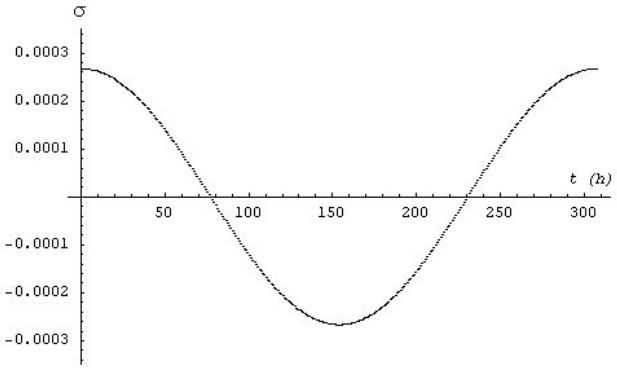

FIGURE 2b. σ. Circular case.

6. Elliptic case

For initial conditions different from those of the circular case there are no simple periodic solutions. We used the astronomical data of July 5^{th}, 2001 to make estimations of initial conditions; the configuration of that date is very close to the configuration of full moon and aphelion.

As we expected, R_1 and σ perform more than 12 oscillations as long as R_2 performs one slow oscillation. Along the numerical integration, the phase locking between R_1 and σ in one lunar cycle is not exact, $\dot{\sigma} \neq 0$ when $R_1 = 0$. For some initial conditions, the phase shift is related with the behavior of R_2, it is negative when R_2 decreases and positive when R_2 increases.

As we have shown in Sec. 4, an orbit that reaches a collinear configuration in an extreme value of R_2 with $P_\sigma = 0$, having started from the *opposite* collinear configuration in an extreme value of R_2 and with $P_\sigma = 0$, is a periodic orbit. Consequently, we have to search for an orbit that starts in full moon and aphelion, and reaches new moon in perihelion, with phase locking orbit will have exactly 13 lunar cycles in one sidereal year.

We call this solution: P-13. The Figs. 3a and 3b show the phase planes R_2, P_2 and σ, P_σ respectively of this orbit. Each point represents an intersection of the orbit with the surface Σ_+.

Making small changes in the energy of the system we can make variations on the period of R_1, this way we find an orbit with an average lunar period of 29.133 days. We call this solution: R-0. Figures (4a) and (4b) show the phase planes R_2, P_2 and σ, P_σ respectively for 39 lunar cycles.

7. Qualitative results

We classified the solutions above mentioned in two categories:

- Quasi-circular orbits. The periodic orbits for the circular and for the elliptic case, show a similar behavior: the Moon describes an oval trajectory centered on Earth, with the maximum distance at first and third quarter. These orbits are very similar to the Hill's periodic solution [6, 9, 10], however we have two different local minima, the higher takes place at full moon, and the lower at new moon. Figure 5 shows the Earth-Moon distance p in a lunar cycle for the orbit P-13.

  In these solutions the Moon orbit around Earth is basically a circular trajectory perturbed by the Sun.

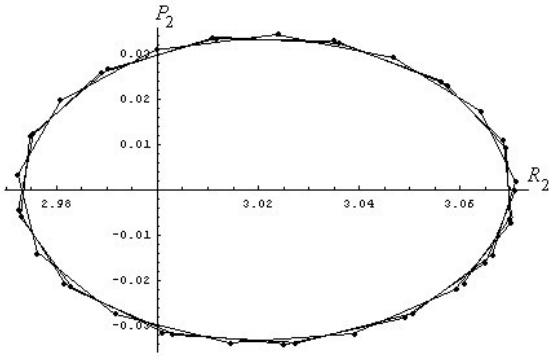

FIGURE 3a. Phase plane R_2, P_2. Elliptic case. Orbit P-13.

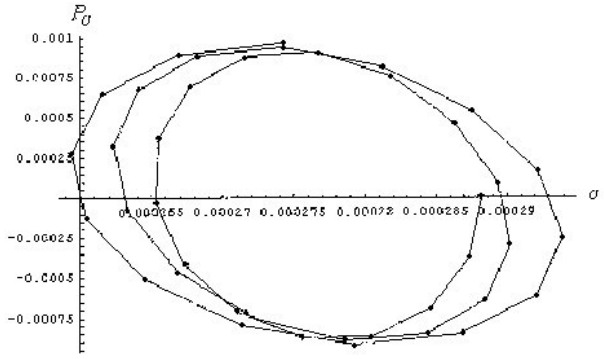

FIGURE 3b. Phase plane σ, P_σ. Elliptic case. Orbit P-13.

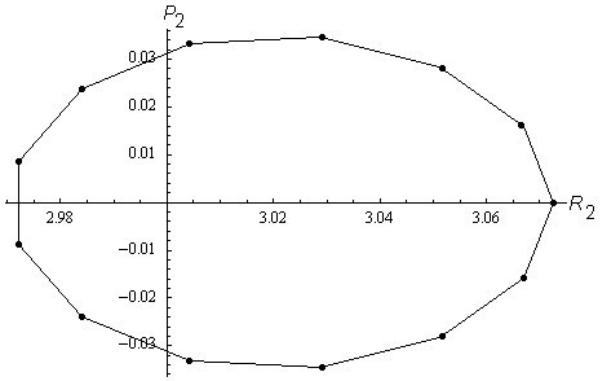

FIGURE 4a. Phase plane R_2, P_2. Elliptic case. Orbit R-0.

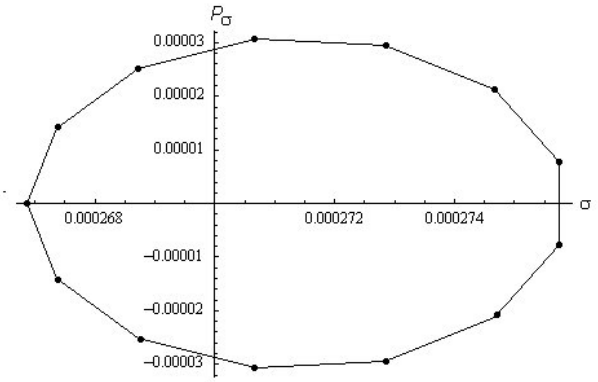

FIGURE 4b. Phase plane σ, P_σ. Elliptic case. Orbit R-0.

- Quasi-elliptical orbits. Perturbing the quasi-circular orbits changing the initial value of σ, but keeping the same energy, we can find solutions with the same period for R_1, in which the Earth-Moon distance has just one maximum and one minimum in a lunar cycle, as it should happen in an elliptical orbit. The amplitude of the oscillations in this case is wider than the amplitude in the quasi-circular case. The extreme values of p are not coupled with the extreme values of R_1 and σ. The orbit R-0 belongs to this category (See Fig. 6).

  In these solutions the Earth-Moon orbit has an own dynamics, independent of the relative position of the Sun.

7.1. Quasi-elliptical orbits

We need to justify this terminus. In an elliptical orbit the Earth-Moon distance p, and the true anomaly θ, must be related by Kepler equation

$$\frac{1}{p} = \frac{1}{\alpha}(1 + \epsilon \cos\theta), \tag{31}$$

where the latus rectum α, and the eccentricity ϵ, related to the energy an angular momentum, are sufficient to characterize the orbit.

Figure 7 shows a graphic of $1/p$ vs. $\cos\theta$ in one lunar cycle for the orbit R-0. Instead of a straight line we have a narrow "tongue" showing that neither the eccentricity nor the latus rectum are constants; in fact, the graphic is different for each lunar cycle. As a qualitative comparing, Fig. 8 shows a similar graphic for the astronomical data of July, 2001; again, we have not a straight line, and we have a different graphic for each month.

In order to compare out numerical solutions with the astronomical data, we make use of the model of rotating Kepler ellipse: Using (31) we can estimate successive values of ϵ and α from the successive extreme values of p:

$$\epsilon = \frac{p_{max} - p_{min}}{p_{max} + p_{min}}, \tag{32}$$

$$\alpha = \frac{2p_{max}p_{min}}{p_{max} + p_{min}}. \tag{33}$$

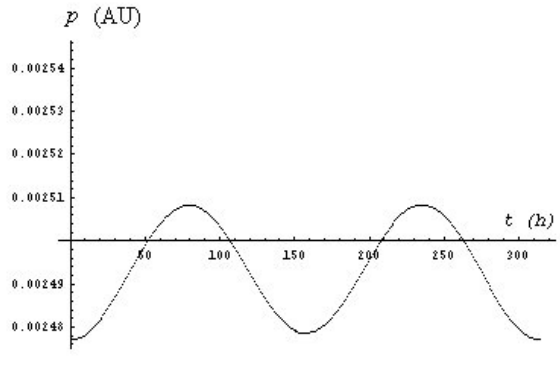

FIGURE 5. p Quasi-circular orbit P-13.

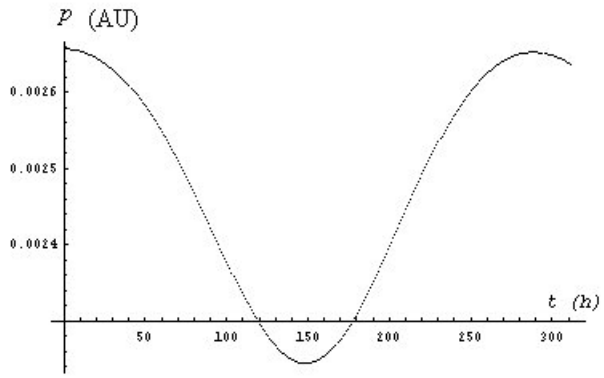

FIGURE 6. p Quasi-elliptical orbit R-0.

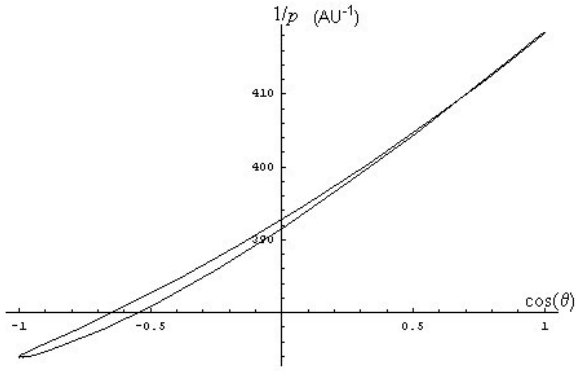

FIGURE 7. Kepler equation. Orbit R-0.

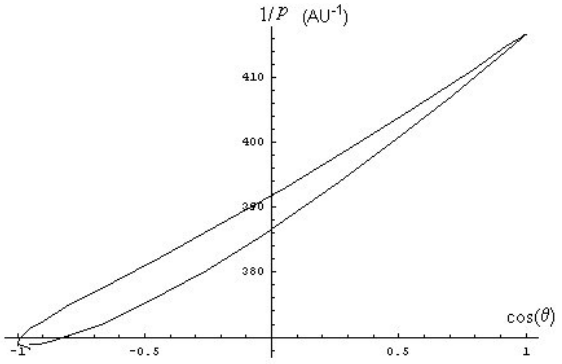

FIGURE 8. Kepler equation. July, 2001.

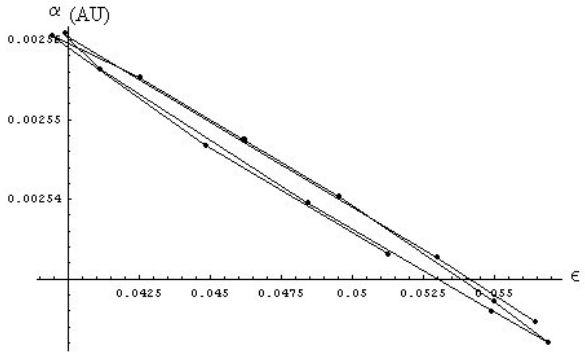

FIGURE 9. ϵ vs α in 13 lunar cycles. Orbit R-0.

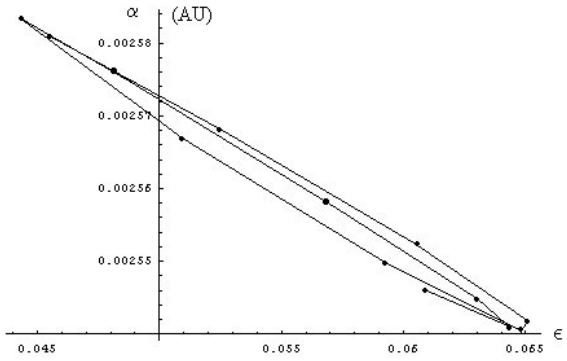

FIGURE 10 ϵ vs α in one year. Astronomical data.

Figure 9 shows a graphic of ϵ against α for thirteen lunar cycles the of the orbit R-0. Other parameters for this orbit are: The average period for θ, the sidereal month, is 26.943 days. The average time between consecutive minima of p, the anomalistic month, is 27.054 days.

Figure 10 shows a similar graphic for the astronomical data from July, 2001 to June, 2002. We can see that both graphics show basically the same behavior: α and ϵ perform approximately two oscillations in a year; one oscillate in opposition to the other, as long α increases, ϵ decreases.

8. Conclusions

The proposed coordinate system seems to be suitable for the study of the Sun-Earth-Moon problem. We made a few approximations in order to simplify the calculus, but they are no essential, so they can be removed. The initial conditions we used are calculated on rough estimations, so we need to get more accurate data in order to adjust or results to the well-known periods of the Moon.

There are other periods of the Moon that we can not get because of the simplification that the system is bidimensional. In future works, we will eliminate this restriction.

Acknowledgements

We want to thank the valuable collaboration of Dr. Joaquín Delgado.

1. A. Escalona Buendía & E. Piña, *Rev. Mex. de Fis.* **47** (2001) 525.
2. E. Piña, *Celest. Mech.* **74** (1999) 163.
3. E. Piña & L. Jiménez-Lara, *Celest. Mech.* **81** (2002) 1.
4. Moshier S. AAv.5.4 Free Software, moshier@na-net.ornl.gov
5. *Astronomical Almanac* (U. S. Government Printing Office, 2001).
6. M. Gutzwiller, *Rev. Mod. Phys.* **70** (1998) 589.
7. E. Piña & L. Jiménez-Lara, *Physica D* **26** (1987) 369.
8. L. Jiménez-Lara & A. Escalona-Buendía, *Celest. Mech.* **79** (2001) 97.
9. D. Brouwer & G. Hori, *Physics and Astronomy of the Moon* (Academic Press, New York, 1962).
10. V. Szebehely, *Theory of Orbits; the Restricted Problem of Three Bodies* (Academic-Press, New York, 1967).